

Impurity and boundary effects in one and two-dimensional inhomogeneous Heisenberg antiferromagnets

P. E. G. Assis, Valter L. L.bero and K. Capelle

Departamento de Física e Informática, Instituto de Física de São Carlos, Universidade de São Paulo,
Caixa Postal 369, 13560-970 São Carlos, SP, Brazil

(Dated: March 23, 2022)

We calculate the ground-state energy of one and two-dimensional spatially inhomogeneous antiferromagnetic Heisenberg models for spins $1/2$, 1 , $3/2$ and 2 . Our calculations become possible as a consequence of the recent formulation of density-functional theory for Heisenberg models. The method is similar to spin-density-functional theory, but employs a local-density-type approximation designed specifically for the Heisenberg model, allowing us to explore parameter regimes that are hard to access by traditional methods, and to consider complications that are important specifically for nanomagnetic devices, such as the effects of impurities, finite-size, and boundary geometry, in chains, ladders, and higher-dimensional systems.

PACS numbers: 71.15.Mb, 75.10.Jm, 75.50.Ee

The study of low-dimensional spin systems is one of the central issues in the physics of correlated electrons. Model Hamiltonians of the Heisenberg type are widely used to study, e.g., antiferromagnetically coupled spin chains, ladders, and layers,^{1,2} and constitute most useful models for strong correlations in undoped cuprates and manganites. Finite-size Heisenberg models, moreover, serve as paradigmatic models for the emerging field of nanomagnetism and spintronics. However, progress in the analysis of nanomagnetic devices requires capability to deal with 'real-life' complications, such as impurities of arbitrary size and location, boundaries of various shapes, and crossovers between finite and extended systems, or between one and higher dimensions. In the present paper we present a convenient and efficient numerical approach for calculating ground-state energies of antiferromagnetic Heisenberg models subjected to such complications.

Traditional numerical methods are well suited for studying generic properties of homogeneous Heisenberg models, and have provided many important insights into the physics of magnetic systems. However, the very significant expenditure of computational effort required by methods such as group-theory-aided exact diagonalization, Quantum Monte Carlo (QMC),³ or the density-matrix renormalization group (DMRG),⁴ imposes rather strict limits on the size and complexity of systems that can be studied. The mean-field approximation can, in principle, be applied to systems of almost arbitrary size and complexity, but its neglect of correlation makes it unreliable as a tool for studying many issues of current physical interest in strongly correlated systems. In *ab initio* calculations, density-functional theory (DFT) provides a convenient and reliable way to go beyond the mean-field (Hartree) approximation, allowing to study real systems of considerable size and complexity.^{5,6,7} While DFT is in principle an exact reformulation of the many-body problem,⁸ its practical implementation requires the use of approximations for the exchange-correlation energy. Among the most important such approximations is the local-density approximation (LDA), the essence of which

is to use the exchange-correlation energy of the uniform electron liquid locally as an approximation to the one of the crystal or molecule of interest.^{5,8} The formal framework of DFT and the LDA is not limited to the *ab initio* case, but can be applied to a large class of model Hamiltonians, too.^{9,10,11,12,13}

In the present paper we study the ground-state energy of one and two-dimensional antiferromagnetic systems with broken translational symmetry, as a function of spin S and system size N . Our choice of symmetry-breaking terms is dictated by complications expected to arise in real nanomagnetic devices, and includes boundaries of diverse geometries, and different types of impurities. Our calculations are performed within DFT for the Heisenberg model,

$$\hat{H} = J \sum_{ij} \hat{S}_i \cdot \hat{S}_j + \sum_i B_i \hat{S}_i; \quad (1)$$

where B_i is a symmetry-breaking magnetic field, coupled to the spins. The simplest local-spin approximation (LSA) for the correlation energy of Hamiltonian (1) reads¹²

$$E_{c;d=1}^{LSA}[\mathbf{S}_i] = 0.36338 J \sum_i \mathcal{F}_i[\mathbf{S}_i] \quad (2)$$

in one dimension, and

$$E_{c;d=2}^{LSA}[\mathbf{S}_i] = 0.316 J \sum_i \mathcal{F}_i[\mathbf{S}_i] \quad (3)$$

in two dimensions. More sophisticated approximations are discussed in Ref. 12. Here $\mathcal{F}_i[\mathbf{S}_i]$ is the modulus of the classical vector \mathbf{S}_i , the ground-state expectation value of the local spin operator \hat{S}_i . The total-energy functional then takes the form

$$E[\mathbf{S}_i] = J \sum_{i,j} \mathbf{S}_i \cdot \mathbf{S}_j + E_c^{LSA}[\mathbf{S}_i] + \sum_i B_i \mathcal{S}_i; \quad (4)$$

where the first term on the right-hand side is the mean-field result, the second the LSA correlation correction to

it, and the last describes the coupling to (possibly spatially varying) magnetic fields. Below we set $B_i = 0$ because we will mostly be interested in intrinsic inhomogeneities such as surfaces and impurities, but both LSA functionals can be applied for nonzero $B_i = 0$ as well. Minimization of $E[S_i]$ with respect to S_i yields the ground-state energy E_0 . Minimization of the first (mean-field) term on its own results in the familiar antiferromagnetic Néel state with alternating up and down spins. For open boundary conditions¹⁴ in one dimension this state has energy $E_{0,d=1}^{MF}(S) = JS^2(N-1)$, while for a two dimensional square lattice $E_{0,d=2}^{MF}(S) = 2JS^2N(N-1)$, where N is the number of sites along the chain and along one side of the square, respectively. E_c^{LSA} provides an additive correction to E_0^{MF} .

First, we consider finite size Heisenberg chains. In Fig. 1 we compare, separately for each spin, the ground-state energies obtained in the mean-field approximation, in LSA, and by exact diagonalization. To be able to compare with exact results we have limited us to fairly small systems, but clearly mean-field and LSA calculations can be performed easily for much larger systems. The LSA is seen to provide substantial improvement on the mean-field results, at negligible extra computational cost. However, we also observe that the LSA does not reproduce the oscillatory structure in the exact results visible for small N , but instead smoothly interpolates through it. As expected on physical grounds,¹² the LSA becomes better as the system size increases.

In these calculations the system is inhomogeneous only due to its finite size. However, the LSA concept can also be applied to spin Hamiltonians in which translational symmetry is broken more radically. Specifically, we now consider an impurity model of much current physical interest: an impurity of spin S_I in a magnetic host material of spin S . This type of model is relevant, e.g., for the analysis of impurities in the antiferromagnetic parent compounds of cuprate superconductors,¹ impurities in correlated spin chains,¹⁵ and recent proposals for quantum computing.^{16,17} Fig. 2 shows the ground-state energy of a spin $1/2$ antiferromagnetic Heisenberg chain, with open boundary conditions, in which one of the boundary spins has been replaced by a spin 1 ion, as schematically indicated in the inset. Mean-field, LSA, and exact values are given. The exact data show that for this type of impurity system the improvement on the mean-field approximation provided by the LSA is of the same order as in the homogeneous case studied in Fig. 1. For comparison purposes we have also included the LSA predictions for an impurity in the bulk, and for a system with two impurities, one in the bulk and one at the surface. Clearly, an antiferromagnetically coupled bulk impurity with $S_I > S$ is energetically more favorable than a surface one, suggesting that self-assembled nanomagnetic systems with this type of impurity will tend to accumulate the impurities in the bulk, and leave the surface homogeneous. The ratio of the energy difference between bulk and surface impurities to temperature is

the controlling parameter for studies of impurity migration. We find that this parameter depends strongly on the impurity spin S_I and system geometry. The extra computational effort for applying the LSA is small, and does not increase significantly if more than one impurity is present, thus opening the possibility to model realistic nanomagnetic systems, with hundreds or thousands of sites, with LSA.

Next, we consider an antiferromagnetic background of spin $S = 1/2$ and varying size, with an impurity of spin $S_I > S$ at the surface. Fig. 3 shows how the combined system background+ impurity approaches the thermodynamic limit for each value of spin S_I . The lowest curve, representing the uniform system, approaches the thermodynamic limit from below, and converges to it rather rapidly. The upper three curves represent the behaviour for different sizes of the impurity spin. The impurity curves approach the thermodynamic limit from above, at a rate that | due to the spin-dependence of the prefactors of the overall $1/N$ decay | decreases with increasing impurity spin. Physically, this behaviour can be understood by noting that for small N the impurity greatly increases the energy of the model as compared to the uniform case, while, as the system size approaches infinity, the influence of the impurity localized at the boundary becomes negligible, and all curves converge to the value $E_0 = JN = 0.432$, close to the value $E_0 = JN = 0.443$ obtained from the Bethe Ansatz for the uniform system.

Next, we turn to the two-dimensional case. Here exact diagonalization becomes prohibitively expensive at even smaller system sizes than in one dimension, and alternative methods, such as DMRG, also encounter very significant difficulties. In Fig. 4 we plot the LSA ground-state energy of finite-size two-dimensional Heisenberg models. These are calculations without impurities, so that the inhomogeneity arises only from the presence of the system boundary, which breaks translational invariance. (As in one dimension, impurities of arbitrary size and location can be added to these systems without a significant increase in computational cost.) Given the LSA functional (3), the generation of the LSA data is a very simple extension of the mean-field calculation. In spite of its simplicity, however, this calculation illustrates an important aspect of LSA: it has the same margin of error in higher dimensions as in one. This is rather untypical of many-body methods, which usually work better in certain dimensionalities (often $d = 1$) than in others.

Finally, we investigate an effect that does not exist in one dimension, namely the dependence of the ground-state energy on the geometry of the system. In Table I we compare the ground-state energies of five Heisenberg models with 100 sites, of shape 1×100 , 2×50 , 5×20 , 10×10 and $2 \times 5 \times 10$. These systems represent, respectively, a one-dimensional chain of the type studied in Fig. 1, a spin ladder with constant coupling along legs and rungs, a multi-legged ladder, a square lattice of the type investigated in Fig. 4, and a representative three-dimensional structure. The data show that: (i) for larger

spins the effect of the system boundary becomes more pronounced. This may be relevant for the study of quantum corrals,¹⁹ and differently shaped magnetic quantum dots. (ii) The higher-dimensional the system, the slower is the convergence to the thermodynamic limit: our result for the 100 site spin $1/2$ chain differs only by 3% from the thermodynamic limit obtained from the Bethe-Ansatz, whereas with the same number of spins the energy of the 10×10 square lattice is about 9% from the thermodynamic limit reported in Ref. 20; a deviation of 3% from this limit is obtained only for a 50×50 lattice. (iii) The step from a chain to a two-legged ladder is much bigger than that from a two-legged ladder to a square lattice, suggesting that in terms of their ground-state energy even small ladders are more similar to extended two-dimensional systems than to chains. (iv) Comparison of the columns 1×100 and 1×100 (2d) shows that simple extrapolation of a higher-dimensional functional to lower dimensionalities results in less negative energies than the correct functional. This observation may also be relevant for *ab initio* calculations applying LDA to low-dimensional systems.

In summary, our results show that the Heisenberg LSA is quantitatively reliable, goes significantly beyond the

mean-field approximation, and allows to calculate the energy of systems of considerable size and complexity. Similar results can be obtained with QMC,³ but at orders of magnitude higher computational cost. (Unlike QMC, DFT is also not limited by a minus-sign problem.) QMC, DMRG and exact data provide benchmarks for testing the quality of improved density functionals. On the other hand, LSA data on the effects of the boundary geometry, the energetic influence of impurities of different sizes and locations, the approach to the thermodynamic limit, and effects of increased dimensionality may be useful information for analysing real nanoscale antiferromagnetic systems, and can also serve as a guide for the application of alternative many-body methods to the same type of system.

Acknowledgments

This work was supported by FAPESP and CNPq. We thank F.C.A. Icaraz and A.M. Alvezzi for useful discussions.

-
- ¹ E. Dagotto, *Rev. Mod. Phys.* **66**, 763 (1994).
 - ² P. Fulde, *Electron Correlations in Molecules and Solids* (Springer, New York, 1991).
 - ³ K.H. Hoglund and A.W. Sandvik, *Phys. Rev. Lett.* **91**, 077204 (2003). A.W. Sandvik, *Phys. Rev. Lett.* **89**, 177201 (2002). K. Harada, N. Kawashima and M. Troyer, *Phys. Rev. Lett.* **90**, 117203 (2003).
 - ⁴ J. Lou, S. Qin, T.-K. Ng, and Z. Su, *Phys. Rev. B* **65**, 104401 (2002).
 - ⁵ W. Kohn, *Rev. Mod. Phys.* **71**, 1253 (1999).
 - ⁶ A.E.M. Mattsson, *Science* **298**, 759 (2002).
 - ⁷ J. Kubler, *Theory of Itinerant Electron Magnetism* (Oxford University Press, Oxford, 2000).
 - ⁸ R.M.D.reizler and E.K.U.G.ross, *Density Functional Theory* (Springer, Berlin, 1990).
 - ⁹ N.A. Lima, M.F. Silva, L.N. Oliveira, K. Capelle, *Phys. Rev. Lett.* **90**, 146402 (2003).
 - ¹⁰ N.A. Lima, L.N. Oliveira, and K. Capelle, *Europhys. Lett.* **60**, 601 (2002).
 - ¹¹ K. Capelle, N.A. Lima, M.F. Silva, and L.N. Oliveira, in *Progress in Theoretical Chemistry and Physics*, eds. N.G. Idopoulos and S.W. Wilson, (Kluwer Academic Publishers, 2003) [also available as cond-mat 0209245].
 - ¹² V.L. Lbero and K. Capelle, *Phys. Rev. B* **68**, 024423 (2003).
 - ¹³ R.J. Magyar and K. Burke, *Phys. Rev. A* **70**, 032508 (2004).
 - ¹⁴ For space reasons we report here only results for open boundary conditions, but all our calculations can be performed for periodic boundary conditions, too.
 - ¹⁵ M. Kenzelmann, G. Xu, I.A. Zaliznyak, C. Broholm, J.F. DiTusa, G. Aeppli, T. Ito, K. Oka, and H. Takagi, *Phys. Rev. Lett.* **90**, 087202 (2003).
 - ¹⁶ A.H. Castro Neto, E. Novais, L. Borda, G. Zarand and I. A. A. de A. eck, *Phys. Rev. Lett.* **91**, 096401 (2003).
 - ¹⁷ D. Loss and D.P. DiVincenzo, *Phys. Rev. A* **57**, 120 (1998).
 - ¹⁸ For $S = 1/2$ the benchmark values for $N < 22$ were obtained by us, by exact numerical diagonalization. For $N = 24$ and 32 they were taken from Ref. 21; for $N = 8$ and $N = 16$ they coincide with those from Ref. 22. For $S = 1$ the benchmark values for $N < 15$ were obtained by us, by exact diagonalization. For $S = 3/2$ and $S = 2$ the benchmark values are estimates extracted from Fig. 1 of Ref. 23.
 - ¹⁹ H.C. Manoharan, C.P. Lutz, and D.M. Eigler, *Nature* **403**, 512 (2000).
 - ²⁰ E. Manousakis *Rev. Mod. Phys.* **63**, 1 (1991).
 - ²¹ S. Li, *J. Chem. Phys.* **120**, 5017 (2004).
 - ²² F.C. Icaraz, M.N. Barber, M.T. Batchelor, R.J. Baxter, and G.R.W. Quispel, *J. Phys. A* **20**, 6397 (1987).
 - ²³ H.Q. Lin, *Phys. Rev. B* **42**, 6561 (1990).

FIG. 1: Ground-state energy of the finite antiferromagnetic Heisenberg chain for various values of the spin S . For each spin, the diamonds represent the mean-field results, the circles are numerically precise benchmark values obtained in independent many-body calculations,¹⁸ the full line is obtained with LSA, and the dashed horizontal line represents the value obtained in the thermodynamic limit, taken from Ref. 4. The LSA is seen to provide significant improvement on the mean-field values, for all S and N .

FIG. 2: Ground-state energy of an antiferromagnetic $S = 1/2$ Heisenberg chain with an $S_I = 1$ impurity at the surface. Horizontal line: mean-field result. Dashed curve: LSA result. Circles: exact values, obtained by numerical diagonalization. Full curve: LSA result for same system, but with the impurity in the bulk. Dash-dotted curve: LSA results for same system, but with two impurities.

FIG. 3: Ground-state energy of an antiferromagnetic $S = 1/2$ Heisenberg chain with different impurities S_I at the boundary. Mean-field values are not included because from Fig. 2 we see that they are much inferior to LSA ones for this system. Crosses: homogeneous system. Diamonds: impurity spin $S_I = 1$, open circles: impurity spin $S_I = 3/2$, full circles: impurity spin $S_I = 2$. The arrow indicates the exact Bethe-Ansatz result $E_0/NJ = -0.443147$.

FIG. 4: Ground-state energy of finite antiferromagnetic Heisenberg square lattices, as a function of spin and system size. Here N stands for the number of sites along the side of the square, hence the total number of sites is N^2 . Dashed curves: mean-field (MF) results. Full curves: LSA results. Full circles: benchmark data obtained by exact diagonalization of small clusters. Arrow: $N \rightarrow 1$ limit, from Ref. 20.

TABLE I: Ground-state energy $E_0=100J$ of antiferromagnetic Heisenberg models of fixed size $N = 100$, and varying geometries and dimensionalities. For each dimensionality we used the proper functional,¹² except in the column labeled 1-100(2d), which contains values obtained for the 1d system with the 2d functional (see discussion in main text).

S	1	100	1	100(2d)	2	50	5	20	10	10	2	5	10
1=2	0.429			0.406	0.528	0.596		0.608				0.696	
1	1.353			1.306	1.796	2.066		2.116				2.491	
3=2	2.795			2.702	3.804	4.412		4.524				5.387	
2	4.687			4.592	6.552	7.632		7.832				9.382	

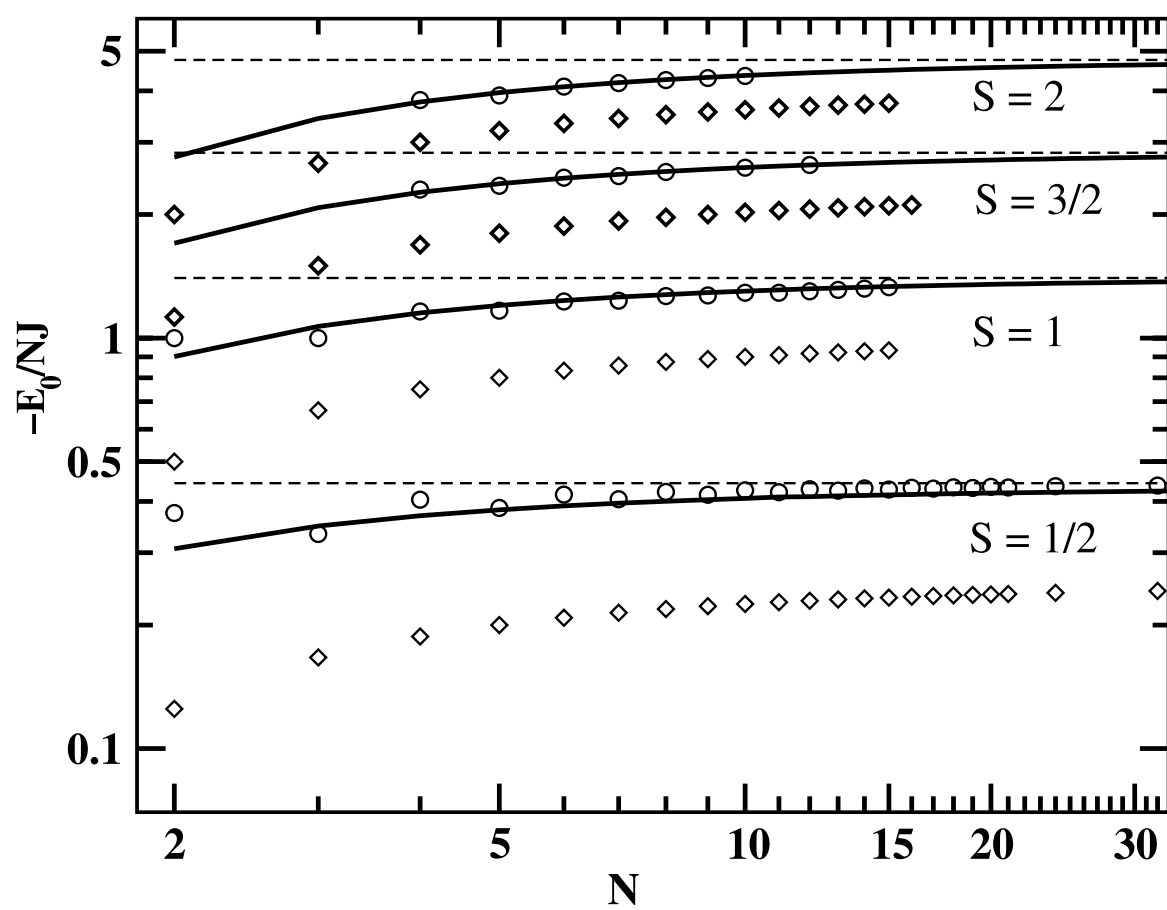


Fig.1

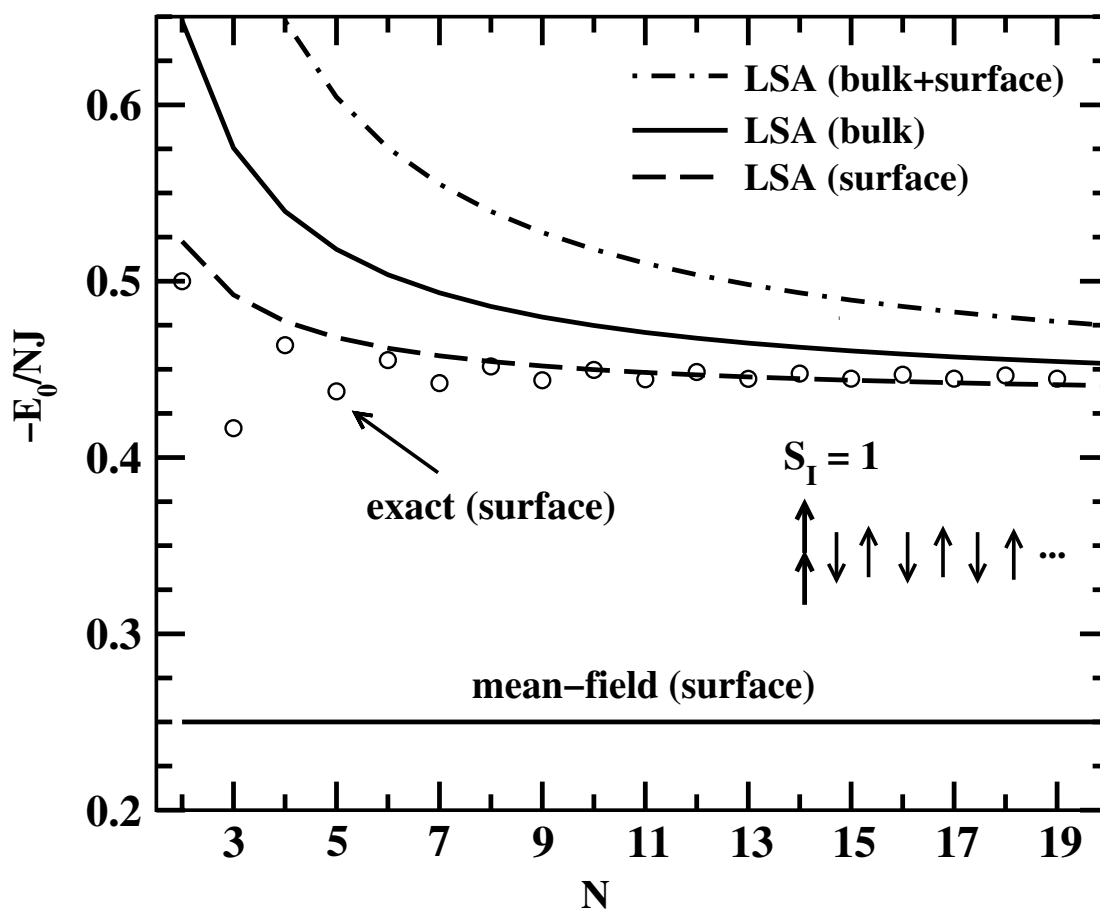


Fig.2

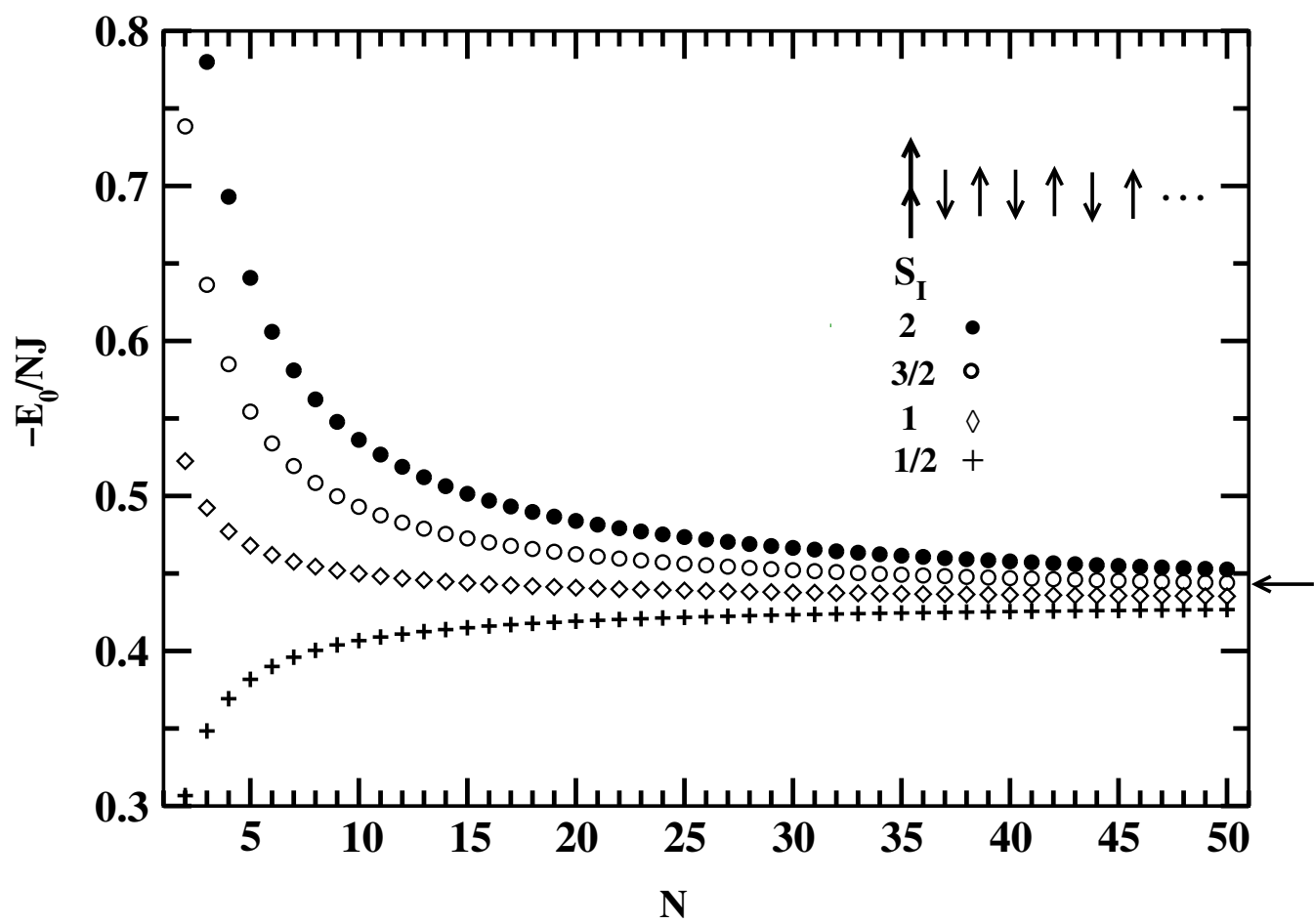


Fig.3

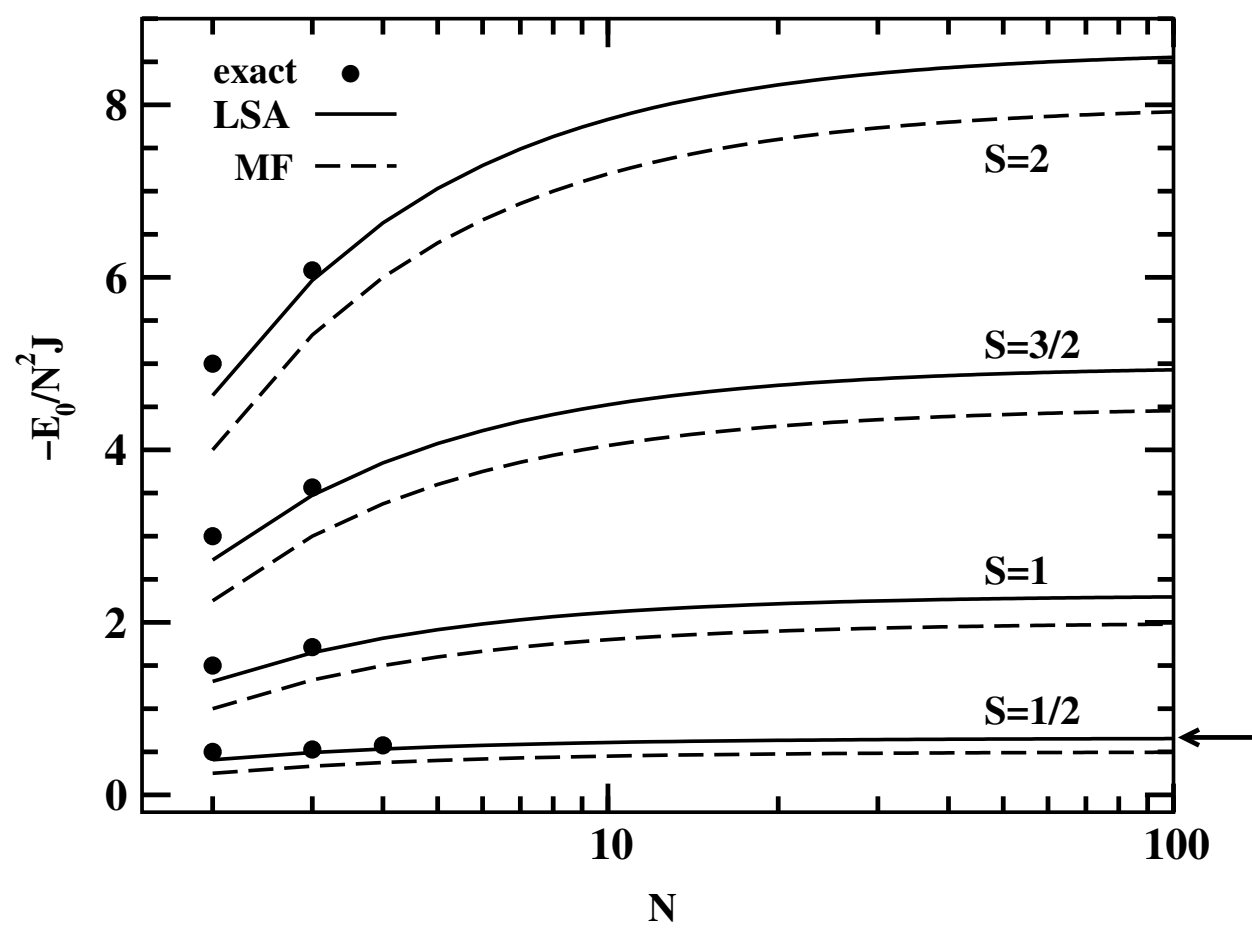


Fig.4